IEEE Access
Multidisciplinary | Rapid Review | Open Access Journal

Received July 30, 2019, accepted August 29, 2019, date of publication September 2, 2019, date of current version September 12, 2019.

Digital Object Identifier 10.1109/ACCESS.2019.2938981

A New Degradation Model for Imaging in Natural Water and Validation Through Image Recovery

YUZHANG CHEN, ZHANGFAN ZENG, AND YONGCAI PAN, (Fellow, IEEE)
School of Computer Science and Information Engineering, Hubei University, Wuhan 430062, China

Corresponding author: Yuzhang Chen (hubucyz@foxmail.com)

This work was supported by the National Natural Science Foundation of China under Grant 61806076, Grant 201710512051, Grant 201810512051 from the Innovation and Entrepreneurship Training Program for College Students in Hubei Province.

ABSTRACT Scattering and turbulence are the main factors affecting imaging in natural water environment. A new model for underwater turbulent degradation is obtained by calculating the scattering transfer factors including the intensity distribution of beam propagation, turbulent fluid medium and suspended particle. In order to verify the proposed model, a controlled laboratory simulation system of turbulent water is established, from which the degradation transfer factor is measured and compared by image restoration and reconstruction. The new model is also applied for field tests in natural ocean water. Experimental results show that based on the proposed model, effect of image restoration and reconstruction can be substantially improved, which proves the correctness and validity of the model.

INDEX TERMS Beam propagation, scattering, underwater turbulence, image restoration, image reconstruction.

I. INTRODUCTION

The light beam transmitted in water will be attenuated due to the absorption and scattering of water. On the other hand, it will change its original transmission direction due to the scattering of suspended particles and turbulence in the water. In the marine environment, water molecules, soluble organic substances, inorganic salts, floating plants and other kinds of suspended particles are the main factors that cause the scattering of light beams. The turbulence existed in water can be regarded as the density fluctuation caused by the random molecular motion, which also has the scattering effect on the beam propagation. As a result, the degradation factors of the turbulent water body mainly include the scattering of the turbulent fluid medium and that of the suspended particles.

The previous degradation models of underwater imaging are based on the absorption and attenuation of water [1], such as Duntley model [2], Voss model [3], Wells small angle approximation model [4]. For studies on the scattering of the turbulent fluid medium, there exist three models used for the calculation of ocean turbulence: the $\kappa - \varepsilon$ model [5], the $\kappa - \kappa L$ model [6] and the GOTM model (General Ocean Turbulence Model) [7]. The above models are mainly aimed at the characteristics of turbulent flow, and it is not aimed at the degradation of underwater imaging. For the study of suspended particle scattering, the theoretical research mainly includes the statistical method [8] and Monte Carlo simulation methods [9]–[11], most of which are experimental measurements, and the main purpose is the inversion of particle size [12], [13]. So there exists no specific model for the degradation of suspended particles in turbulence.

In recent years, the research on underwater image restoration has mostly focused on the application of mathematical methods such as depth neural network to image processing [14]–[21]. Studies on degenerate models mainly includes: Professor Hou and his colleagues proposed and studied the degradation model [22]–[24] and image restoration [25], [26]of undersea turbulence in various ocean imaging environments; Mohua [27] proposed a new image formation model for image restoration; In my previous papers, the underwater imaging degradation model based on beam propagation is also established for obtaining the point spread function (PSF) [28]. In above models, particle scattering and path radiance are commonly obtained as constant or measured factors. As a result, the new model is dedicated to the study of scattering of suspended particles and fluid in turbulent water bodies.

In this paper, a new degradation model is proposed, which considers the scattering degradation factors of beam propagation, turbulent fluid medium and suspended particle. In order

The associate editor coordinating the review of this article and approving it for publication was Qiangqiang Yuan.

to verify the correctness and validity of the model, a water imaging experiment platform was built, modulation transfer function (MTF) was measured and applied to image restoration and reconstruction algorithms [29], the result of which were compared and analyzed. Finally, field tests in sea water were carried out for further verification.

II. THEORY

Considering the turbulence as an optical system, the optical transfer function of underwater imaging system can be obtained by calculating the scattering transfer factors including beam propagation, turbulent fluid medium and the suspended particle.

A. BEAM PROPAGATION TRANSFER FACTOR

The distribution of light field and intensity in the three-dimensional rectangular coordinate system on the imaging plane can be expressed as [19]:

$$E_m(x,y,z) = i^m c_m A^2 \left(\frac{z}{r^2}\right)^2 \left(\frac{\Gamma^2}{\Gamma^2+x^2}\right) exp\left(-\frac{2y^2}{\Omega^2}\right) H_m\left(\frac{\sqrt{2}}{\Omega}y\right) \tag{1}$$

$$I_0(x,y,z) = \sum_{m=0}^{m} E_m(x,y,z) E_m^*(x,y,z) \tag{2}$$

where $\Gamma^2 = (pr/k)^2$, $\Omega^2 = 4q^2r^2/k^2$, $p = 1/w_{0x}$, $q = 1/w_{0y}$, w_{0x}, w_{0y} denote the waist widths of beams in fast and slow axes, k is wave numbers in vacuum, $k = 2\pi/\lambda$, r is distance from observation point to origin coordinate. H_m is the Hermits term, order of which is determined by the actual measured intensity distribution, c_m is Weighting factor and A is the constant amplitude factor.

For a stack consisting of several light sources, the light intensity distribution will change due to the correction of the directivity factor of the array:

$$I_r(x,y,z) = \sum_{i=1}^{n} I_i\{(y-\Delta y_i) * cos\theta\} \tag{3}$$

where Δy_i and θ denote the position and angle shift of array intensity distribution relative to the principal optical axis.

Then the degradation transfer factor of beam propagation can be calculated by:

$$MTF_{beam} = \frac{\pi \mathcal{F}(I_r/I_{r=0})}{4} \tag{4}$$

B. TURBULENT FLUID MEDIUM TRANSFER FACTOR

The general form of turbulent fluid medium degradation transfer function can be expressed by the following equation [30]:

$$MTF_{tur} = MTF_{opt} \exp[-\frac{1}{2}W(\lambda f)] \tag{5}$$

where MTF_{opt} denotes the Modulation Transfer Function of optical system, λ is optical wavelength, f is spatial angular frequency, and $W(\lambda f)$ denotes the turbulent wave structure function.

The Modulation Transfer Function of optical system can be calculated by the diffraction limit of optics and nonlinear distortion of sensors [31]:

$$MTF_{opt} = \frac{2}{\pi}[\arccos\frac{f}{f_o} - \frac{f}{f_o}\sqrt{1-(\frac{f}{f_o})^2}] * \frac{\sin(\pi \times dp \times f)}{\pi \times dp \times f} \tag{6}$$

where $f_o = \frac{Dp}{\lambda}$ is the optical cut off frequency at the image plane, Dp is the diameter of the lens, dp is the size of pixels.

Considering the underwater turbulence as a homogeneous isotropic transmission medium, the wave structure function of the optical wave propagating in the underwater turbulence to the distance of d can be expressed as [32]:

$$W(\lambda f) = 8\pi\mu^2 d \int_0^{\infty} [1 - J_0(\alpha\eta)\psi(\alpha,l,L)]\alpha d\alpha \tag{7}$$

where $\mu = 2\pi/\lambda$ is the wave number of the transmission of waves, $J_0(\alpha\eta)$ is the zero order Bessel function, α is spatial wave number, η denotes the diameter distribution on the plane of vertical direction of transmission at distance d, $\psi(\alpha, l, L)$ is a simplified von Karman refractive index spectrum, and its expression is [32]:

$$\psi(\alpha,l,L) = 0.0165\alpha^{-11/3}[\exp(-\frac{\varepsilon^2}{(5.92/l)^2}) + 1 - \exp(-\frac{\alpha}{(2\pi/L)^2})] \tag{8}$$

where l and L denotes the inner and outer scales of turbulence respectively.

Using the combined hyper geometric function solutions of wave structure function, we can get the final expression of Eq.5 as the turbulent fluid medium degradation factor:

$$\begin{aligned} MTF_{tur} &= MTF_{opt} \exp < -\frac{1}{2}\{1.73[\eta^{5/3} \\ &\quad - 2.98(\frac{2\pi}{L})^{-5/3}\frac{5\eta^2(2\pi/L)^2}{24} \\ &\quad + 2.98(\frac{5.92}{l})^2\frac{6}{5\Gamma(5/6)}(\frac{\eta^2(5.92/l)^2}{4})^{5/6}]\} > \\ &= \frac{2}{\pi}[\arccos\frac{f}{f_o} - \frac{f}{f_o}\sqrt{1-(\frac{f}{f_o})^2}] * \frac{\sin(\pi \times dp \times f)}{\pi \times dp \times f} \\ &\quad * \exp\{-0.865[(\frac{fD_p}{f_0})^{5/3} - 0.62(\frac{2\pi}{L})^{1/3}(\frac{fD_p}{f_0})^2 \\ &\quad + \frac{2.38}{\Gamma(5/6)}(\frac{fD_p}{f_0})^{5/3}]\} \end{aligned} \tag{9}$$

where Γ is the combined hyper geometric function.

C. SUSPENDED PARTICLE TRANSFER FACTOR

Regarded the tiny suspended particles in the water body as homogeneous spherical particles, the Stokes vector of the scattering and absorption of a single particle is [33]:

$$S = [\mathrm{I\ Q\ U\ V}]^{\mathrm{T}} \tag{10}$$

where S denotes the Stokes vector, I is the total light intensity, Q, U and V are the different directions and types of polarization respectively.

Based on the Mueller matrix, the vector relation between the incident light and the scattered light can be expressed as:

$$S_s = M_{4\times4} \times S_i \tag{11}$$

where S_i and S_s denotes the Stokes vector of the incident light and the scattered light, $M_{4\times4}$ is the Mueller matrix including 16 elements.

The expression of the Mueller matrix can be written as [32]:

$$M_{4\times4} = \frac{F_{4\times4}}{\mu^2 d^2} = \frac{1}{\mu^2 d^2} \cdot \begin{bmatrix} F_{11} & F_{12} & 0 & 0 \\ F_{12} & F_{22} & 0 & 0 \\ 0 & 0 & F_{33} & -F_{34} \\ 0 & 0 & F_{34} & F_{33} \end{bmatrix} \tag{12}$$

where d is the imaging distance from observer to scattering point, μ is the wave number, $F_{4\times4}$ is the transformation matrix.

The size and location of suspended particles with a certain concentration in turbulent water follow the law of random distribution, each of which is not coherent; as a result, the scattering of suspended particles group can be seen as linear superposition of single particle scattering, which can be calculated by using the statistical method. The corresponding scattering matrix can be calculated by:

$$S_{4\times4} = \begin{bmatrix} S_{11} & S_{12} & 0 & 0 \\ S_{12} & S_{22} & 0 & 0 \\ 0 & 0 & S_{33} & -S_{34} \\ 0 & 0 & S_{34} & S_{33} \end{bmatrix} = \frac{4\pi \int_{r_1}^{r_2} F_{4\times4} n(r) dr}{\eta^2 \int_{r_1}^{r_2} \sigma_s n(r) dr} \tag{13}$$

where $S_{4\times4}$ is the volume scattering matrix, each element of which denotes the relative change amount of amplitude and phase from incident light to scattering light, r is the radius of suspended particle, r_1 and denotes r_2 the lower and upper bounds of the particle radius respectively, $n(r)$ is the particle size distribution, σ_s denotes the particle scattering cross section.

The incident light in the scattering plane of the azimuth angle of φ can be divided into two vibration components along the X axis and the Y axis, the parallel vibration component Exi and the vertical vibration component Eyi of which can be expressed by [34]:

$$\begin{aligned} E\text{hi} &= \cos\varphi Exi + \sin\varphi Eyi \\ E\text{vi} &= \sin\varphi Exi - \cos\varphi Eyi \end{aligned} \tag{14}$$

The Stokes vector of Ehi is (1,1,0,0), while the Stokes vector of Evi is (1, -1,0, 0). The intensity of light is the square of the amplitude, so we have:

$$\begin{aligned} I_{\text{hs}} &= (S_{11} + S_{12}) I_{hi} \\ &= (S_{11} + S_{12}) \left|\cos\varphi Exi + \sin\varphi Eyi\right|^2 \\ I_{\text{vs}} &= (S_{11} - S_{12}) I_{vi} \\ &= (S_{11} - S_{12}) \left|\sin\varphi Exi - \cos\varphi Eyi\right|^2 \end{aligned} \tag{15}$$

where S_{11}, S_{12} are Muller matrix elements.

The scattered light intensity in the specific scattering direction can be expressed by:

$$I_s(\theta, \varphi) = I_{\text{hs}}(\theta, \varphi) + I_{\text{vs}}(\theta, \varphi) \tag{16}$$

As a result, the volume scattering function of suspended particles can be calculated as:

$$\begin{aligned} \beta(\theta, \varphi) = {} & (S_{11} + S_{12}) \left|\cos\varphi Exi + \sin\varphi Eyi\right|^2 \\ & + (S_{11} - S_{12}) \left|\sin\varphi Exi - \cos\varphi Eyi\right|^2 \end{aligned} \tag{17}$$

The broadening pulse time caused by the scattering of particles can be calculated by the following formula [35]:

$$\delta T = \text{t1} - \text{t0} = \frac{1}{c}\{\frac{1/3}{s \cdot d \cdot \theta_0^2}[(1 + 2sd\theta_0^2)^{3/2} - 1] - 1\} \tag{18}$$

where c is the speed of light in water; d is the transmission distance, s is the scattering coefficient of the water body; θ_0 denotes the root mean square scattering angle of the phase function which can be calculated as follows:

$$\theta_0 = (\int_0^{\pi} \theta^2 \cdot \frac{\beta(\theta, \varphi)}{s} d\theta)^{1/2} \tag{19}$$

The time broadening of the light beam can be regarded as the point spread distance, which is the point spread function (PSF) after normalization, and the MTF can be calculated by the Fourier transform of the PSF:

$$\begin{aligned} & MTF_{\text{par}} \\ & = F(PSF_{\text{par}}) = \text{F}\left(\log_{10}(\pi(\text{c} \cdot \delta T)^2)\right) \\ & = \text{F}\left(\log_{10} < \pi(\{\frac{1/3}{s \cdot d \cdot \theta_0^2}[(1 + 2sd\theta_0^2)^{3/2} - 1] - 1\})^2 >\right) \end{aligned} \tag{20}$$

Then the total MTF of the turbulent degradation can be expressed as:

$$MTF_{image} = MTF_{beam} \cdot MTF_{par} \cdot MTF_{tur} \tag{21}$$

The formulas for calculating the three MTF components are Equations 4, 9, and 20.

The PSF of the imaging system can be obtained from the MTF by Hankel transform in the form of [36]:

$$h = 2\pi \int J_0(2\pi\theta\varphi) MTF_{image}(\varphi) \varphi d\varphi \tag{22}$$

where θ is the spatial angle, φ is the spatial frequency, J_0 is the Bessel function.

Using PSF as prior knowledge, the main principle of the blind restoration and total variation regularization super-resolution reconstruction can be generally described as the

following iterative equations which is studied by previous works [31], [37]:

$$\min_f J(f) = \min_f (\frac{1}{2} \left\| f * h - f^{'} \right\|^2 + \sigma J_\sigma(f)) \quad (23)$$

$$f_{n+1} = P[f_n + \sum_{i=1}^{j} \lambda P(g_i - hf_i)] \quad (24)$$

where $f^{'}$ and f represent the observation image and the original image respectively, h is the PSF of the system which can be derived from the proposed model, $*$ is the convolution operation. The purpose of restoration is to solve f from the equation. To solve this problem, the point spread function can be used as a priori knowledge and regularization technique as a constraint. $J_\sigma(f)$ is the penalty factor. Eq.23 is a regularized algorithm to end iteration. If the algorithm is applied directly and alone, the image will be restored. If the algorithm is applied to eq.24, it will be part of the super-resolution reconstruction. f_{n+1} and f_n are the iteration results of the n+1th and nth iterations, g_i is the observed low resolution image sequence, λ is the simple operator, f_i is the starting estimate which can be obtained by interpolation, $i = 1, 2, \ldots$ j is the number of limit sets, P is the projection operator. The g_i is interpolated to form f_i, then the point spread function h and f_i are computed by Convolution Multiplication to simulate g_i, and the set is formed by recording the closest points of g_i and hf_i. Then, the h is iterated over the high-resolution mesh f_n to finish the iteration by regularization.

III. EXPERIMENTS AND DISCUSSION

A. CONTROLLED LABORATORY SIMULATION

A laboratory turbid water environment with controlled simulated turbulence is established for experiments. The experimental system consists of a water pump as power, a flow meter and other equipment connected with a water tank to form a water circulation system. Experimental suspended particles are added into the tank water to form turbidity. The 532nm green semiconductor laser is used as light source with spot size of 10-20mm; CMOS (Complementary Metal Oxide Semiconductor) image sensor is used to capture underwater turbulence images. The experimental water tank is made of high-transmittance acrylic plates, in order to allow more than 90% of the laser source to shine on the target plate. The size of the water tank is $1.5\text{m} * 0.5\text{m} * 0.5\text{m}$, and the two ends are provided with a water inlet and a water outlet with a cross section size of $0.04\text{m} * 0.04\text{m}$ to connect the water pump and the flow meter respectively, a circulating pump with a maximum lift of 5m and a maximum flow of 7.8m^3/h is used to provide water power.

A turbulent flow will be produced when the inlet flow reaches a certain speed. The laser and CMOS image sensors are packaged under water and arranged with the target board at the two ends of the long side of the water tank respectively. The structure and photograph of experimental system are shown in Fig.1 and Fig.2. The physical properties for calculating PSF are listed in Table. 1.

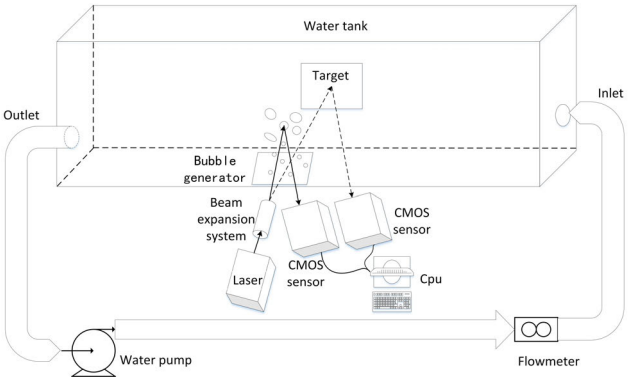

FIGURE 1. Structure diagram of experimental system.

FIGURE 2. Photograph of experimental system.

TABLE 1. Physical properties of experimental system.

Parameters	Value
Water attenuation	2.5m^{-1}
LD power	200mW
Operating Voltage	12V
Angle of viewing	160°
Distance between LD and CCD	1cm
Imaging distance d	5m
The diameter of the lens D_p	0.05m
scattering coefficient s	0.0638m^{-}

The water pump drives the flow of water, and the water valve controls the size of the water flow, Then the flow meter can read the flow velocity in real time, and then calculate the turbulent Reynolds number and turbulence intensity. The target images used are sinusoidal fringe images with frequency of various lines, the vertical stripes in the center of which is used for obtaining MTF information, while the horizontal stripes are for calibrating the shot angle and height of the camera. Line number of sine fringe marked in the center of the target is used to check the results of the experiment. The MTF of an optical system can be calculated as the ratio of the modulation of the image and the object at a given spatial

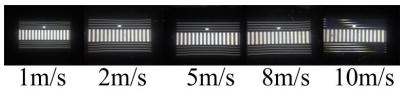

FIGURE 3. Sample images used for measuring MTF.

frequency which is calculated by the maximum and minimum values of the light intensity [26].

Image decomposition through multi-channel wavelet transform is applied, in which appropriate wavelet basis is chosen according to the turbulence model. The low-frequency part of image is simplified using matrix theory, then restored by iterative blind restoration equation using PSF as prior knowledge, while edge information of the high-frequency part is enhanced by the optimization algorithm, and then the wavelet reconstruction is processed with the restored low frequency part.

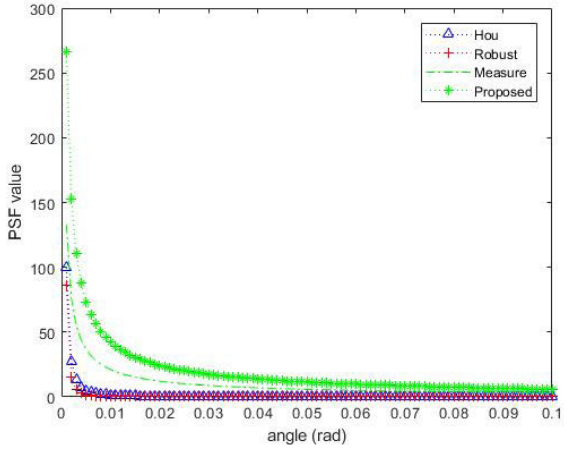

FIGURE 4. The PSF curves of underwater models.

PSF is calculated and applied as prior knowledge in image processing, the correlation curve is shown in the Fig. 4.

When the water velocity of the inlet is 5 m/s, the target object is photographed 60 times by CCD sensor in 5 seconds, the captured image sequences are processed and compared. Based on the measured MTF [26] and proposed model in this paper, the processing results of image restoration and super resolution reconstruction algorithms are shown in Fig.6. The core algorithm for restoration is blind deconvolution algorithm, and that for super resolution reconstruction is total variation POCS (Projections onto Convex Sets) algorithm. Meanwhile, Hou's model [25], the Robust model [38], are also added to the comparative experiments. When the water velocity of the inlet is 20 m/s, the original captured sample image and processed results are shown in Fig.7 and Fig.8.

Peak Signal to Noise Ratio (PSNR) and structural similarity index (SSIM) are selected as the evaluation criteria for the images compared with the clear images on the shore of the target board. At the same time, blind, objective image quality metrics are applied to evaluate the performance of the image enhancement algorithms [39]. According to the

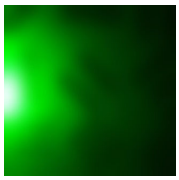

FIGURE 5. Original captured image of underwater object (size 2766×2074 pixels).

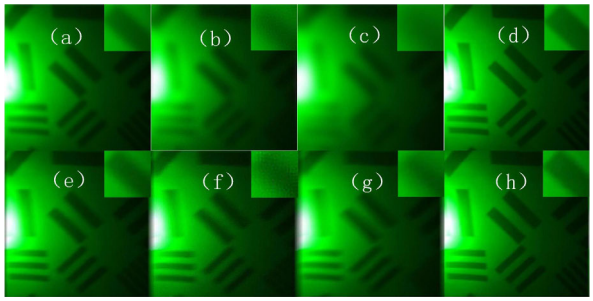

FIGURE 6. Restoration results (size 2766×2074 pixels) by: (a) Hou's model (HOU), (b) robust model ROB), (c) measured model (MEA), (d) proposed model (PRO), and reconstruction results (size 4608×3456 pixels) by: (e) Hou's model (HOU), (f) robust model ROB), (g) measured model (MEA), and (h) proposed model (PRO).

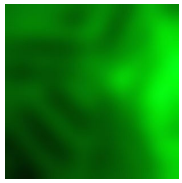

FIGURE 7. Original captured image of underwater object (size 2766×2074 pixels).

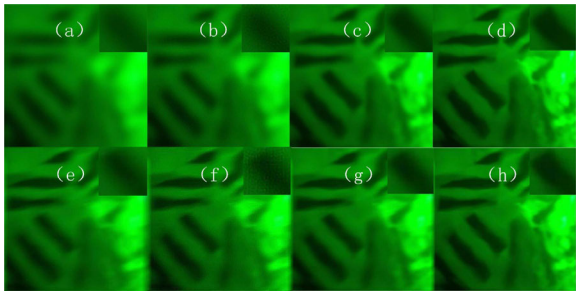

FIGURE 8. Restoration results (size 2766×2074 pixels) by: (a) Hou's model (HOU), (b) robust model ROB), (c) measured model (MEA), (d) proposed model (PRO), and reconstruction results (size 4608×3456 pixels) by: (e) Hou's model (HOU), (f) robust model ROB), (g) measured model (MEA), (h) proposed model (PRO).

characteristics of image restoration and image reconstruction, the blur metric (BM) [28], [31], the gray mean grads (GMG), and Laplacian sum (LS) [28] are chosen. The smaller the BM value means clearer image, while higher the GMG and LS values means the higher image quality. The evaluation results of Fig.6 and Fig.8 are shown in Table.2 and Table.3. The processing time of the algorithms are shown in Table.4.

TABLE 2. Evaluation results of Fig.6.

	original	HOU-restore	ROB-restore	MEA-restore	PRO-restore	HOU-reconstruct	ROB-reconstruct	MEA-reconstruct	PRO-reconstruct
PSNR		29.5036	33.1132	35.6463	28.2928	26.6004	26.2771	25.9613	27.2153
SSIM		0.728	0.317	0.177	0.910	0.422	0.532	0.647	0.967
BM	0.4206	0.3810	0.3920	0.4036	0.3509	0.3171	0.3197	0.3329	0.3049
GMG	10241012	13173602	11831102	11184708	13432532	13667751	13576334	13547935	14053643
LS	1848700	2563694	2207908	2063282	2723188	3044623	2960923	2895226	3218829

TABLE 3. Evaluation results of Fig.8.

	original	HOU-restore	ROB-restore	MEA-restore	PRO-restore	HOU-reconstruct	ROB-reconstruct	MEA-reconstruct	PRO-reconstruct
PSNR		34.7414	31.9950	28.1794	26.9788	26.8623	26.7367	26.5977	26.4258
SSIM		0.218	0.417	0.898	0.874	0.339	0.378	0.423	0.802
BM	0.3715	0.3459	0.3328	0.3252	0.3289	0.3056	0.2780	0.2716	0.2720
GMG	10272720	13324805	14272136	15655282	15982358	17119593	17233211	17332789	17366048
LS	1826588	2446192	2669415	3057583	3258692	3504167	3579074	3670958	3806477

TABLE 4. Comparison of algorithm running time (min).

	HOU-restore	ROB-restore	MEA-restore	PRO-restore	HOU-reconstruct	ROB-reconstruct	MEA-reconstruct	PRO-reconstruct
Fig.6	2.5	11.2	3.5	5.2	3.1	15.6	3.6	10.1
Fig.8	2.6	12.5	1.3	6.1	3.1	10.3	3.6	9.3

From the subjective point of view, in the case of restoration in micro-turbulence, the Hou model and the model proposed in this paper perform better than the other two models, in which robust model has a serious ringing effect. Because Robust model is also proposed by our group, it is found that this method can only be applied to the degradation caused by the beam transmission, but cannot solve the turbulence problem. In the case of restoration in strong turbulence, the Hou model also does not perform well. But the model based on measurement and the model proposed in this paper have better performance. In the case of reconstruction, the model based on measurement and the model proposed in this paper have better performance both in micro and strong turbulence circumstances.

From the values of PSNR and SSIM, in the case of restoration in micro-turbulence, robust model also has the lowest values, while the Hou model has the highest values, which is slightly higher than the proposed model. In the case of restoration in strong turbulence, the proposed model has the

FIGURE 9. Original captured image of underwater object in shallow sea water (size 2766×2074 pixels).

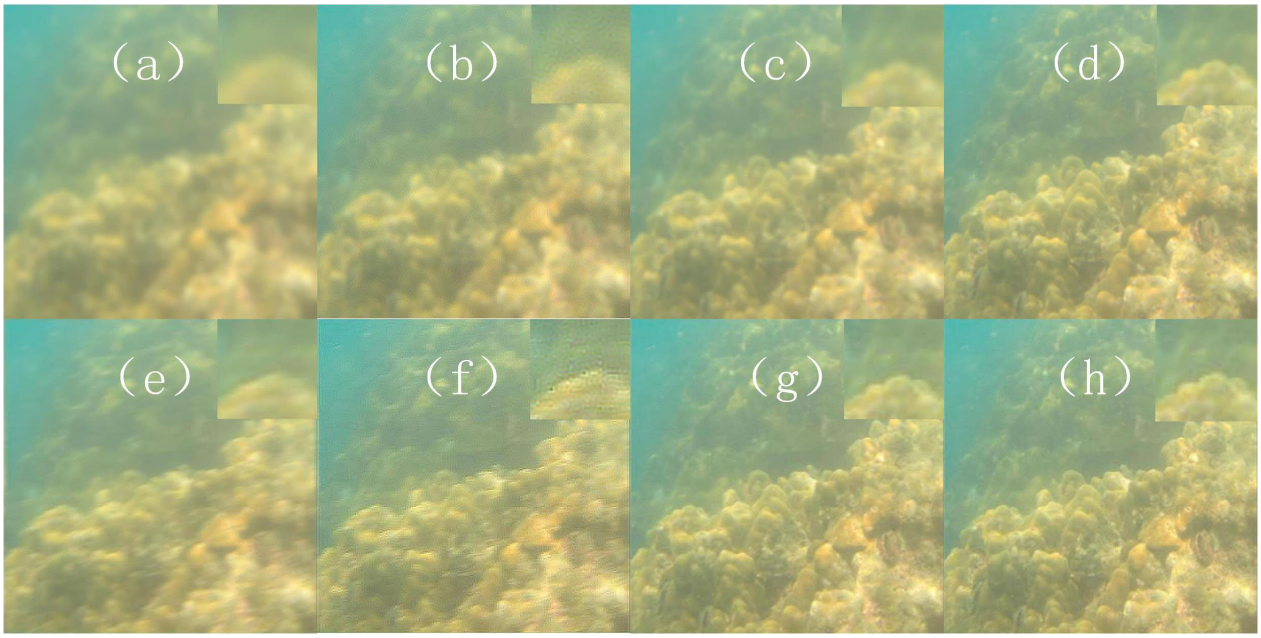

FIGURE 10. Restoration results (size 2766×2074 pixels) by: (a) Hou's model (HOU), (b) Robust model ROB), (c) Measured model (MEA), (d) Proposed model (PRO), and reconstruction results (size 4608×3456 pixels) by: (e) Hou's model (HOU), (f) Robust model ROB), (g) Measured model (MEA), (h) Proposed model (PRO).

highest values which is slightly higher than the Hou model. In the case of reconstruction in micro-turbulence, both the measured model and proposed model performs better than other two models, while in the case of strong turbulence, only the proposed model performs better.

In addition, it is found that the proposed method has advantages in SSIM, but it has limitations in PSNR, which is found to be the influence of image noise. If the image is denoised firstly, the value of PSNR will be significantly improved. Therefore, the proposed model has a low tolerance to noise.

From the perspective of other evaluation indicators, the clearness by image restoration can be seen in the BM values of restored results, in which the restoration using measured model performs best, the effect of proposed model is also better than the Hou and robust model.

The magnification enhancement by image super resolution reconstruction can be seen in the GMG and LS values, in which the reconstruction using proposed model performs best.

From the above experimental results, we can see that robust model cannot be applied to turbulence degradation, Hou model can be applied to micro-turbulence, and measured model can be applied to strong turbulence. The model proposed in this paper can be applied to both micro-turbulence and strong turbulence circumstances.

As can be seen from Table 4, Hou's model and measurement-based model are faster while the Robust model is the slowest. The proposed model is slower, but within the acceptance range. Since the focus of this paper is on the validity of the model, the speed of the algorithm will be further studied for practical use in the future.

FIGURE 11. Original captured image of underwater object in deep sea water (size 2766×2074 pixels).

As a result, the PSF calculated by proposed model can effectively enhance the performance of image restoration and reconstruction, and shows advantage compared to other models, which verifies the correctness and effectiveness of the proposed model.

B. FIELD TESTS IN OCEAN WATER

The MTF of nature water can be measured by the turbulent velocity field using a Particle Image Velocimetry (PIV) method in which small bubbles are seeded into the water as non-polluting tracing particles. The velocity field distribution in the flow field can be obtained by auto correlation and cross-correlation algorithms using flow particle images captured in the vertical direction of laser beam which illuminating a thin film layer in the flow field [40].

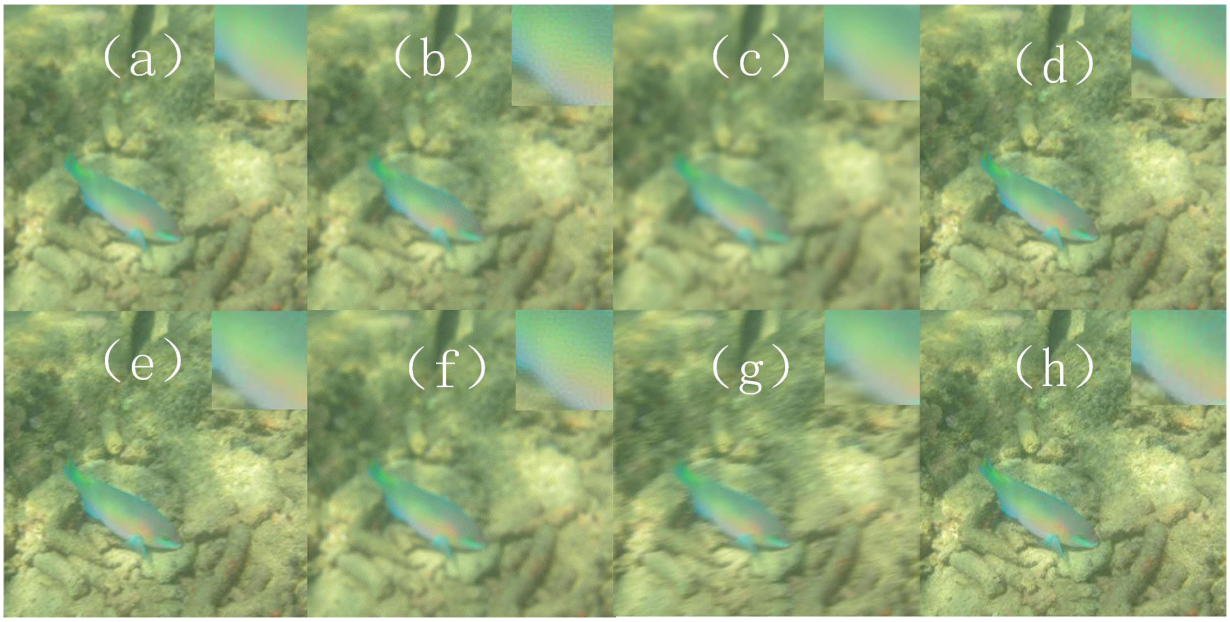

FIGURE 12. Restoration results (size 2766×2074 pixels) by: (a) Hou's model (HOU), (b) robust model ROB), (c) measured model (MEA), (d) proposed model (PRO), and reconstruction results (size 4608×3456 pixels) by: (e) Hou's model (HOU), (f) robust model ROB), (g) measured model (MEA), and (h) proposed model (PRO).

TABLE 5. Evaluation results of fig.10.

	original	HOU-restore	ROB-restore	MEA-restore	PRO-restore	HOU-reconstruct	ROB-reconstruct	MEA-reconstruct	PRO-reconstruct
BM	0.4806	0.4763	0.4284	0.4148	0.4419	0.3791	0.3260	0.2834	0.2255
GMG	13662971	15937056	17571103	19872152	23419762	20980315	21596532	24252638	24802167
LS	2435348	3018483	3495569	4250214	5690684	4665826	4939963	6616789	6951660

TABLE 6. Evaluation results of fig.12.

	original	HOU-restore	ROB-restore	MEA-restore	PRO-restore	HOU-reconstruct	ROB-reconstruct	MEA-reconstruct	PRO-reconstruct
BM	0.5844	0.5235	0.5382	0.5705	0.5154	0.3721	0.4210	0.4775	0.2944
GMG	24341987	35029919	30631997	27883573	39107105	38639369	35478108	34531252	41576561
LS	4567258	8492024	6706100	5707759	10469208	11978600	9438683	8812788	14382405

The experimental data were obtained by an underwater imaging system which consists of a LD laser operated at 532-nm as light source, and two CMOS sensor as image sensor, in which one sensor is used for capturing the images of bubbles, while the other one for the images of underwater object, the bubbles was generated by bubble generator at a distance of 0.5m from laser and CMOS sensor.

In order to verify the practical role of the proposed model, MTF based restoration and reconstruction algorithms are applied to the images captured in ocean with turbulence. The original image obtained in Shallow South China Sea and enhanced images are shown in Fig.9 and Fig.10, while the sample image captured in deep sea and its processing results are shown in Fig.11 and Fig.12.

TABLE 7. Comparison of algorithm running time (min).

	HOU-restore	ROB-restore	MEA-restore	PRO-restore	HOU-reconstruct	ROB-reconstruct	MEA-reconstruct	PRO-reconstruct
Fig.6	3.1	12.3	5.2	9.6	2.8	10.5	6.9	10.4
Fig.8	2.4	11.5	4.9	5.2	1.2	10.5	4.7	6.9

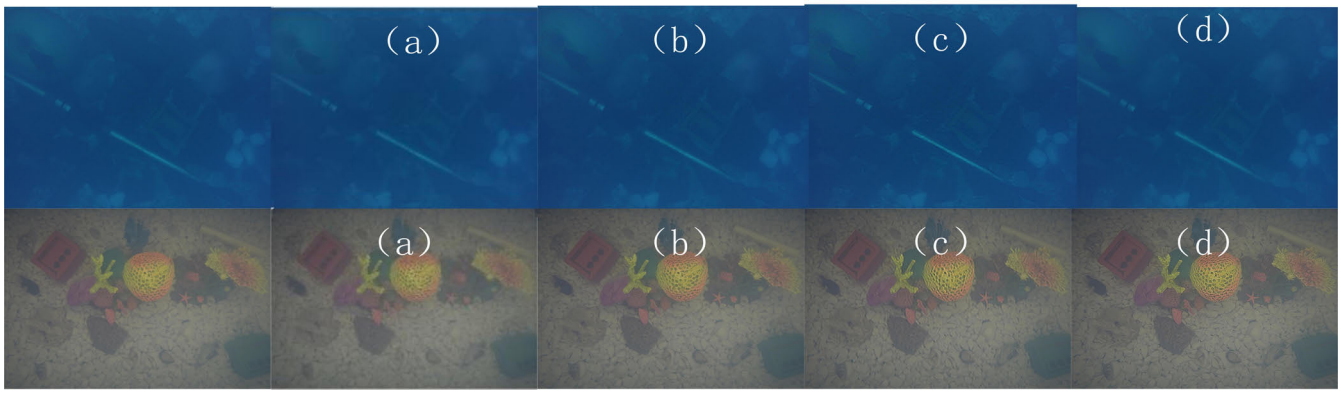

FIGURE 13. Original images and Restoration results (size 3630×2723 pixels) by: (a) Hou's model (HOU), (b) robust model ROB), (c) measured model (MEA), (d) proposed model (PRO).

As there is no clear picture of the target board, only BM, GMG and LS can be used as evaluation criteria. The evaluation results of Fig.10 are shown in Table.5, while that of Fig.12 are shown in Table.6. The processing time of the algorithms are shown in Table.7.

From the subjective and objective point of view, the restoration and reconstruction results of shallow sea are similar to those of strong turbulence, while that of deep sea are similar to those of micro-turbulence.

As can be seen in Table.5 and Table.6, The proposed model also shows effective improvement in image quality.

In order to further verify the validity of the model, two sets of the TURBID Dataset [41] with the turbidity of I_{10} are used for image restoration. The processing results are shown in Fig.13 and evaluation results are shown in Table.8.

TABLE 8. Evaluation results of fig.13.

		HOU-restore	ROB-restore	MEA-restore	PRO-restore
Deep blue	PSNR	18.0834	42.1475	12.3454	44.2948
	SSIM	0.189	0.739	0.143	0.893
Milk	PSNR	27.9462	44.7823	18.5591	43.9233
	SSIM	0.277	0.801	0.544	0.823

It can be seen from the experimental results that Hou's model and measured model are inferior, and the proposed model and Robust model show good results, especially in the Deep blue data set, the effect of proposed model is better than other models. This is because the data set is mainly produced for turbidity. According to the paper of the dataset, the generation of turbidity mainly affects the scattering. Therefore, the Robust model for light scattering and the proposed model considered particle scattering will achieve better recovery effects. The Hou model for turbulence and the measured model dependent on measured parameters cannot achieve good results. The model proposed in this paper can be used for both turbulence and particle scattering conditions, so it is more applicable.

The new model can provide guidance on how to mitigate the effects of turbulence impacts on underwater imaging in various turbulent environments.

IV. CONCLUSION

The presented effort proposed a new degradation model for underwater imaging, including the beam propagation transfer factor calculated by intensity distribution, turbulent fluid medium transfer factor calculated by wave structure function and the suspended particle scattering transfer factor calculated by Muller matrix. The experiments are conducted in turbulent water of both controlled laboratory simulation and natural environments. The degradation transfer function is measured in laboratory simulation and compared with the theoretical model by their application in image restoration and reconstruction. The result of comparison shows that in

laboratory and field tests, the model proposed in this paper show advantages in both micro-turbulence and strong turbulence circumstances. The model proposed in this paper has broad application prospects in underwater exploration, geomorphological detection and water quality researches.

REFERENCES

[1] H. Lu, Y. Li, Y. Zhang, M. Chen, S. Serikawa, and H. Kim, "Underwater optical image processing: A comprehensive review," *Mobile Netw. Appl.*, vol. 22, no. 6, pp. 1204–1211, 2017.

[2] S. Q. Duntley, "Underwater lighting by submerged lasers and incandescent sources," Scripps Inst. Oceanogr. Visibility Lab., Univ. California, San Diego, CA, USA, 1971.

[3] K. J. Voss, "Simple empirical model of the oceanic point spread function," *Appl. Opt.*, vol. 30, no. 18, pp. 2647–2651, 1991.

[4] W. H. Wells, "Loss of resolution in water as a result of multiple small-angle scattering," *J. Opt. Soc. Amer.*, vol. 59, no. 6, pp. 686–691, Jun. 1969.

[5] B. E. Launder and D. B. Spalding, *Lectures in Mathematical Models of Turbulence*. Salt Lake City, UT, USA: Academic, 1972.

[6] G. L. Mellor and T. Yamada, "Development of a turbulence closure model for geophysical fluid problems," *Rev. Geophys.*, vol. 20, no. 4, pp. 851–875, 1982.

[7] H. Burchard, K. Bolding, and M. Ruiz-Villarreal, "GOTM, A general ocean turbulence model: Theory, implementation and test cases," Eur. Commission, Brussels, Belgium, Tech. Rep. EUR 18745 EN, 1999.

[8] M. I. Mishchenko, A. A. Lacis, and L. D. Travis, *Scattering, Absorption, and Emission of Light by Small Particles*. Cambridge, U.K.: Cambridge Univ. Press, 2002, no. 4, p. 494.

[9] S. Bartel and A. H. Hielscher, "Monte Carlo simulations of the diffuse backscattering Mueller matrix for highly scattering media," *Appl. Opt.*, vol. 39, no. 10, pp. 1580–1588, 2000.

[10] M. Xia, K. Yang, X. Zhang, J. Rao, Y. Zheng, and D. Tan, "Monte Carlo simulation of backscattering signal from bubbles under water," *J. Opt. A, Pure Appl. Opt.*, vol. 8, no. 3, pp. 350–354, 2006.

[11] M. Xu, "Electric field Monte Carlo simulation of polarized light propagation in turbid media," *Opt. Express*, vol. 12, no. 26, pp. 6530–6539, 2004.

[12] G. E. Fernandes, Y.-L. Pan, R. K. Chang, K. Aptowicz, and R. G. Pinnick, "Simultaneous forward- and backward-hemisphere elastic-light-scattering patterns of respirable-size aerosols," *Opt. Lett.*, vol. 31, no. 20, pp. 3034–3036, 2006.

[13] H. Tan, R. Doerffer, T. Oishi, and A. Tanaka, "A new approach to measure the volume scattering function," *Opt. Express*, vol. 21, no. 16, pp. 18697–18711, 2013.

[14] C.-H. Yeh, C.-H. Huang, and C.-H. Lin, "Deep learning underwater image color correction and contrast enhancement based on hue preservation," in *Proc. IEEE Underwater Technol. (UT)*, Apr. 2019, pp. 1–6.

[15] C. Sánchez-Ferreira, L. S. Coelho, H. V. H. Ayala, M. C. Q. Farias, and C. H. Llanos, "Bio-inspired optimization algorithms for real underwater image restoration," *Signal Process., Image Commun.*, vol. 77, pp. 49–65, Sep. 2019.

[16] Z. Zhang and X. Yang, "Reconstruction of distorted underwater images using robust registration," *Opt. Express*, vol. 27, no. 7, pp. 9996–10008, 2019.

[17] Y.-T. Peng and P. C. Cosman, "Underwater image restoration based on image blurriness and light absorption," *IEEE Trans. Image Process.*, vol. 26, no. 4, pp. 1579–1594, Apr. 2017.

[18] S.-B. Gao, M. Zhang, Q. Zhao, X.-S. Zhang, Y.-J. Li, "Underwater image enhancement using adaptive retinal mechanisms," *IEEE Trans. Image Process.*, vol. 28, no. 11, pp. 5580–5595, Nov. 2019.

[19] J. Y. Chiang and Y.-C. Chen, "Underwater image enhancement by wavelength compensation and dehazing," *IEEE Trans. Image Process.*, vol. 21, no. 4, pp. 1756–1769, Apr. 2012.

[20] J.-L. Yin, B.-H. Chen, and Y. Li, "Highly accurate image reconstruction for multimodal noise suppression using semisupervised learning on big data," *IEEE Trans. Multimedia*, vol. 20, no. 11, pp. 3045–3056, Nov. 2018.

[21] J.-L. Yin, Y.-C. Huang, B.-H. Chen, S.-Z. Ye, "Color transferred convolutional neural networks for image dehazing," *IEEE Trans. Circuits Syst. Video Technol.*, to be published.

[22] W. Hou, S. Woods, W. Goode, E. Jarosz, and A. Weidemann, "Impacts of optical turbulence on underwater imaging," *Proc. SPIE*, vol. 8030, no. 1, pp. 307–316, 2011.

[23] W. Hou, S. Woods, E. Jarosz, W. Goode, and A. Weidemann, "Optical turbulence on underwater image degradation in natural environments," *Appl. Opt.*, vol. 51, no. 14, pp. 2678–2686, 2012.

[24] W. Hou, E. Jarosz, S. Woods, W. Goode, and A. Weidemann, "Impacts of underwater turbulence on acoustical and optical signals and their linkage," *Opt. Express*, vol. 21, no. 4, pp. 4367–4375, 2013.

[25] A. V. Kanaev, W. Hou, S. R. Restaino, S. Matt, and S. Gładysz, "Restoration of images degraded by underwater turbulence using structure tensor oriented image quality (STOIQ) metric," *Opt. Express*, vol. 23, no. 13, pp. 17077–17090, 2015.

[26] S. Matt, W. Hou, W. Goode, and S. Hellman, "Introducing SiTTE: A controlled laboratory setting to study the impact of turbulent fluctuations on light propagation in the underwater environment," *Opt. Express*, vol. 25, no. 5, pp. 5662–5683, 2017.

[27] M. Zhang and J. Peng, "Underwater image restoration based on a new underwater image formation model," *IEEE Access*, vol. 6, pp. 58634–58644, 2018.

[28] Y. Chen and K. Yang, "MAP-regularized robust reconstruction for underwater imaging detection," *Optik*, vol. 124, no. 20, pp. 4514–4518, 2013.

[29] N. Wang, H. Zheng, and B. Zheng, "Underwater image restoration via maximum attenuation identification," *IEEE Access*, vol. 5, pp. 18941–18952, 2017.

[30] M. Haindl and S. Šimberová, "Probabilistic model-based restoration of short-exposure astronomical images," in *Proc. IASTED*, 2004, pp. 1–6.

[31] Y. Chen and J. Chen, "Spatial adaptive regularized MAP reconstruction for LD-based night vision," *Optik*, vol. 125, no. 13, pp. 3162–3165, 2014.

[32] M. Wang, Z. Zhao, S. Wang, and R. Ji, "Restoring method for underwater degraded images based on improved turbulence model and polarization imaging," *Trans. Chin. Soc. Agricult. Eng.*, vol. 29, no. 25, pp. 203–209.

[33] M. I. Mishchenko, L. D. Travis, and A. A. Lacis, *Scattering, Absorption, and Emission of Light by Small Particles*, 2002, no. 4, p. 494.

[34] M. E. Lee and M. R. Lewis, "A new method for the measurement of the optical volume scattering function in the upper ocean," *J. Atmos. Ocean. Technol.*, vol. 20, no. 4, pp. 563–571, 2003.

[35] H. E. Xi shun *et al.*, *Research on the Transmission Delay of Laser Pulse Caused by the Sea Water Scattering Effects*. Beijing, China: Chinese Publisher, 2001.

[36] Y. Z. Chen, H.-Y. Tan, W.-L. Yang, Y. Yang, N. Hao, and K.-C. Yang, "Iterative back projection reconstruction for underwater imaging," *Lasers Eng.*, vol. 34, pp. 287–302, Jul. 2016.

[37] Y. Chen, L. Yang, Z. Zeng, Q. Ren, X. Xu, Q. Zhang, T. Xu, and S. Ouyang, "Degradation in LED night vision imaging and recovery algorithms," *Optik*, vol. 144, pp. 240–245, Sep. 2017.

[38] Y. Chen, W. Yang, H. Tan, Y. Yang, N. Hao, and K. Yang, "Image enhancement for LD based imaging in turbid water," *Optik*, vol. 127, no. 2, pp. 517–521, 2016.

[39] W. Hou and A. D. Weidemann, "Objectively assessing underwater image quality for the purpose of automated restoration," *Proc. SPIE*, vol. 6575, Apr. 2017, Art. no. 65750Q.

[40] R. J. Adrian, "Twenty years of particle image velocimetry," *Experim. Fluids*, vol. 39, no. 2, pp. 159–169, Aug. 2005.

[41] A. Duarte, F. Codevilla, J. De O. Gaya, and S. S. C. Botelho, "A dataset to evaluate underwater image restoration methods," in *Proc. OCEANS*, 2016, pp. 1–6.

YUZHANG CHEN was born in 1984. He received the bachelor's, master's, and Ph.D. degrees from the Huazhong University of Science and Technology. He is an Associate Professor and the master's Tutor with the School of Computer and Information Engineering, Hubei University.

He has been involved in research on photoelectric imaging detection, photoelectric information perception, image processing, and the embedded development for a long time. His main research contents include laser and LED in water, night vision or underwater scattering medium radiation transmission theory and computer simulation, image acquisition and restoration and reconstruction algorithms, and image processing algorithms embedded including the research of Android development.

ZHANGFAN ZENG received the B.S. degree in communication engineering from Wuhan University, China, the M.S. degree in communication engineering from The University of Manchester, U.K., and Ph.D. degree in communication engineering from the University of Birmingham, U.K., in 2006, 2007, and 2013. Since December 2015, he has been a full-time Associate Professor with Hubei University, China. He has published over 20 research articles. He holds one patent in radar community. His research areas include wireless communication and digital signal processing.

YONGCAI PAN is currently a Full Professor and the Head of Laboratory of Signal Processing and System Analysis with Hubei University. His research interests include wireless communication, signal processing, and intelligent systems. He has extensive exposure and experience in industrial projections.